Two-thirds of agricultural carbon and biodiversity loss occurs on one-third of the agricultural area

Supplementary information

Baoxiao Liu [1,*], Paul Behrens [1,2], Zhongxiao Sun [3], Laura Scherer [1]

1. Institute of Environmental Sciences (CML), Leiden University, 2333 CC, Leiden, the Netherlands.
2. Oxford Martin School, University of Oxford, Oxford OX1 3BD, United Kingdom
3. College of Land Science and Technology, China Agricultural University, 100193, Beijing, China.

* Baoxiao Liu. Email: b.liu@cml.leidenuniv.nl

This file includes:

1. Supplementary methods
2. Comparisons with other work
3. Figures S1-10
4. Tables S18-19 (For Tables S1-17, please refer to the Supplementary xlsx file)

Global agricultural land We include cropland and pasture as agricultural land and did not account for other land demands related to the agricultural sector, such as housing, manufacturing, processing, and transportation. We use cropland spatial data from CROPGRIDS[1], a novel synthesis of the most recently available information on harvested and physical area maps for 173 crops for 2020, at a global spatial resolution of 0.05° (approximately 5.6 km at the equator). We used physical area maps of CROPGRIDS. We aggregated 173 crop maps to one global cropland map (Fig. S1a). Pasture distribution is from HILDA+ pasture/rangeland map[2], which is built from several land cover datasets (grassland), combined with the Gridded Livestock of the World-2010 (GLW3) map and calibrated with FAO statistics. The HILDA+ source maps are at 0.6 arcmin spatial resolution with the cell value representing the land use category. We extracted grid cells defined as "pasture/rangeland" and converted them into units of area (hectare), assuming the whole area in each grid cell is used for pasture. We harmonized the global pasture map derived from HILDA+ with the aggregated cropland map by resampling to 3 arcmin and capping the area of grid cells in pasture if the sum of the area of pasture and cropland exceeds the cell size. This harmonization reduced the total pasture area by 0.71 Mkm^2, ~2% of the original total area in HILDA+ (30.03 Mkm^2). The harmonized global pasture map is shown in Fig. S1b.

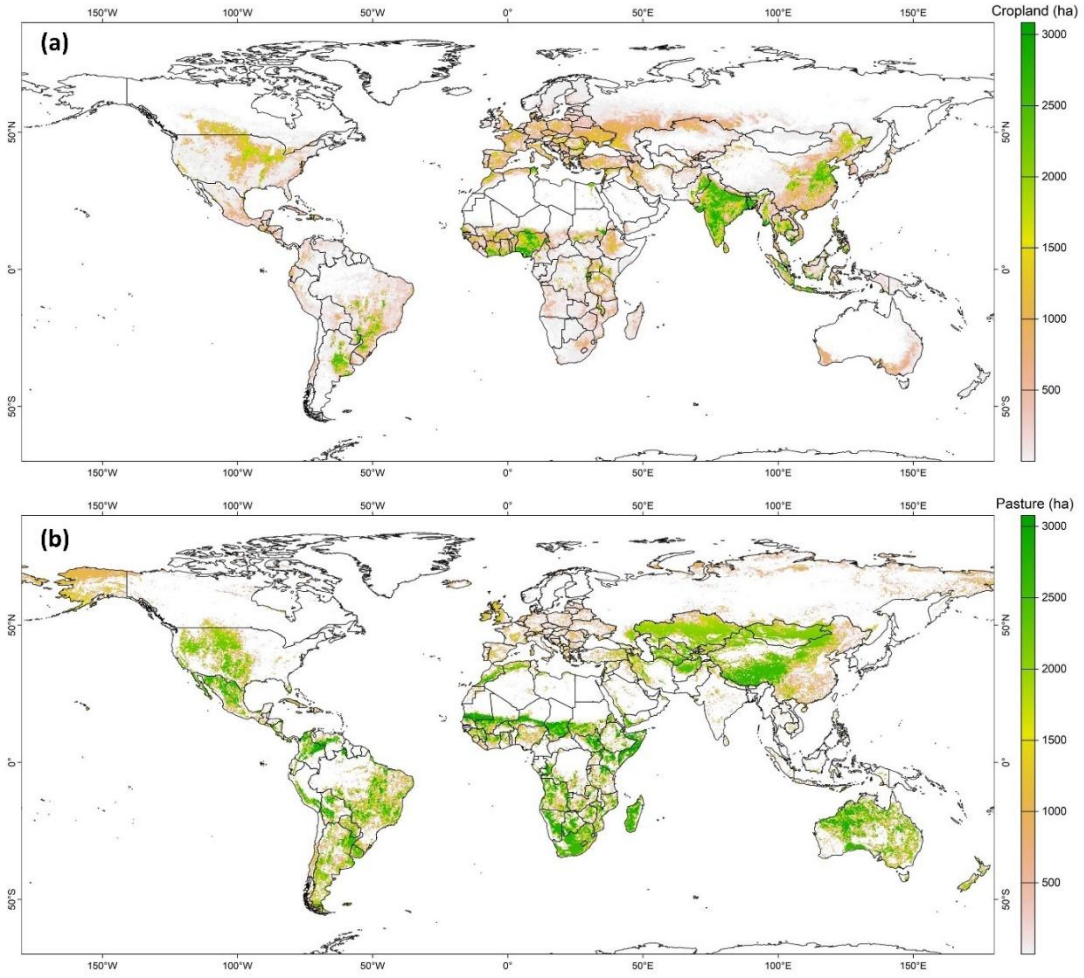

Fig. S1. Global cropland area (a) and pasture area (b). Spatial resolution: 3 arcmin; Unit: ha

Carbon loss density Here, we account for carbon loss in biomass and soil. We produced the biomass carbon loss density map for agriculture for 2019, using Eq.1-2. The actual biomass carbon stock data (C_{2019} , C_{2000}) is from Xu et al.[3], which provided annual estimates (ranging from 2000 to 2019) of global terrestrial living biomass (in Mg C ha^{-1}) based on synthesizing ground-based forest inventories with airborne and satellite data. To derive C_{hypo}, we used Eq. 2 by combining the carbon density map for the year 2000 (C_{2000}) with the potential-actual biomass carbon reduction percentage map (C_{redu_2000}) from Erb et al[4], which used circa 2000 data. We disaggregated the coarser grid cells in these maps to 3 arcmin, assuming homogenous carbon density and reduction in each cell.

$$C_{loss2019} = C_{hypo} - C_{2019} \quad (1)$$

$$C_{hypo} = C_{2000}/(1 - C_{redu\_2000}) \quad (2)$$

In some grid cells, we found carbon gains. That is, the current carbon storage is larger than the potential storage due to current agricultural inputs and the natural productivity of that land. This happens in 14% of grid cells globally but the sum of all those cells with carbon gains in agriculture is only 0.66 Pg C. Because we focused on carbon loss only, we excluded the grid cells with carbon gains by setting those cells to zero, following Walker et al.[5]. In addition, we capped the cell values in the biomass carbon loss map to 47.9 kg C m^{-2}, as it is the maximum potential biomass stock density value of undisturbed vegetation[4]. The capping reduced the total biomass carbon loss in agriculture for 2019 by 8.39 Pg C. We masked the biomass carbon loss map with global agricultural area extent derived from previous steps to obtain biomass carbon loss in agriculture (Fig. S2a).

We accounted for carbon loss in soil as the changes between current soil carbon pool and the predicted pool without land use loss, similar as we did for biomass carbon. Prior global studies[6–9] have assumed loss of 25% of soil carbon within the top meter of soils during the conversion of natural ecosystems to croplands. For conversion to pastures, Searchinger et al.[7] assume no change in soil carbon for tropical pastures and a 10% loss of soil carbon in temperate pastures. However, such uniformed percentages are not able to account for the soil loss variation across space, which is of great importance in a global mapping study as presented here.

We first obtained a soil loss density map combining the 2010 soil organic carbon stocks (Mg C / ha) for 0-100 cm depths and projected soil organic carbon stocks without land use also for the top meter from Sanderman et al.[10]. Again, we removed cells with soil carbon gains, which were related to ~16% cells and 5.30 Pg C soil carbon gains in agriculture. Because we used different cropland and pasture maps from Sanderman et al.[10], we only considered the soil carbon loss within the global agricultural area extent derived in our study. We produced a soil carbon loss map for agriculture at 3 arcmin (Fig. S2b), also assuming homogenous soil carbon loss happens in each larger cell. We assume there is no soil carbon loss nor gains since 2010 given the lack of more recent data. We aggregated biomass and soil carbon loss to obtain the total carbon loss in agriculture at 3 arcmin resolution (Fig. S2c).

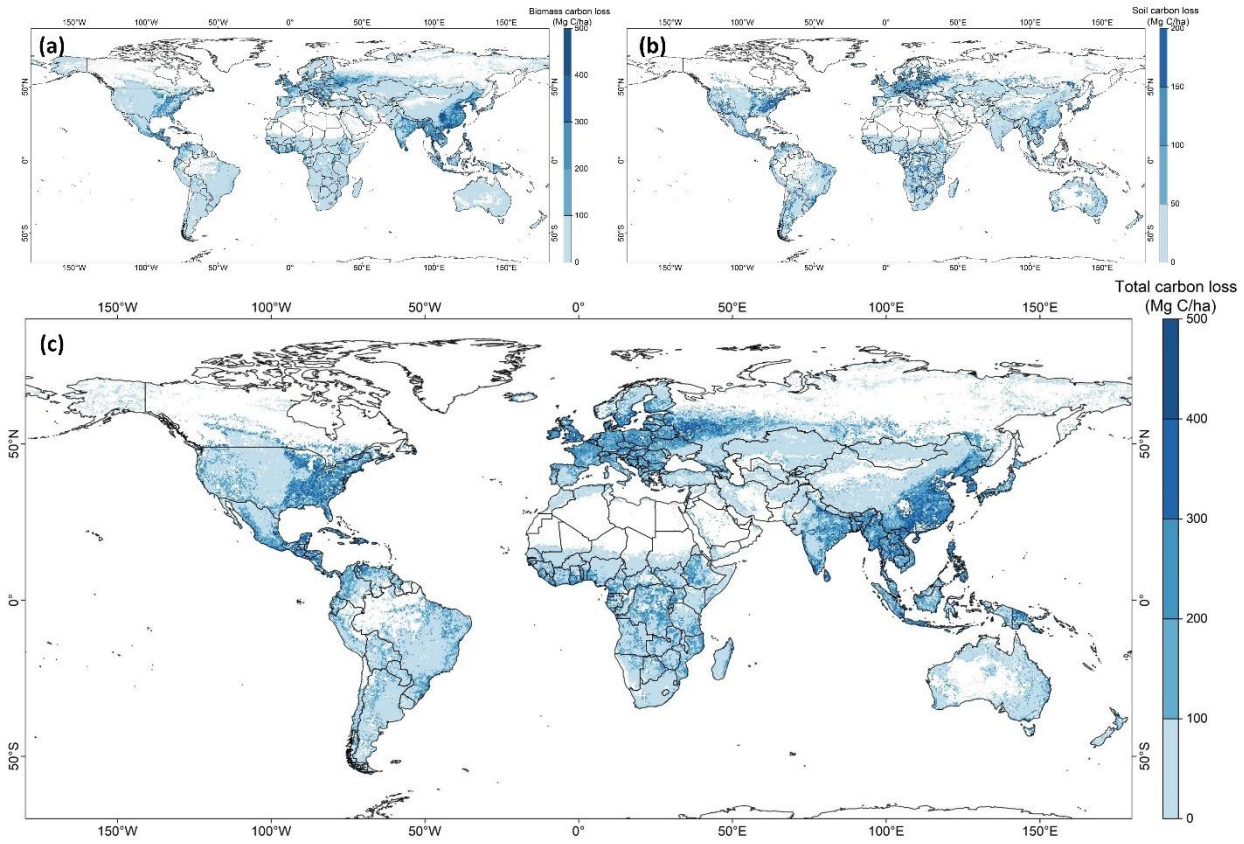

Fig. S2. Carbon loss in biomass (a), soil (b) and total carbon pool, including biomass and soil (c) in agricultural areas. Spatial resolution: 3 arcmin; Unit: Mg C/ha.

Land use intensity and biodiversity loss density To quantify land use intensity in cropland, we followed the methods in Scherer et al.[11] using land management inputs (irrigation and fertilizer N & P) as the indicators. Specifically, the global irrigation map (AEI) is from Mehta et al.[12]. Global nitrogen (N) and phosphorus (P) fertilizer use maps are obtained from Lu & Tian[13]. We assigned land-use intensity levels to cropland area (Fig. S1a) by overlaying it with AEI, N and P use maps. If the area equipped for irrigation and both fertilizer uses did not exceed the first quantile of non-zero values, we consider it minimal use. If the area equipped for irrigation or any of the fertilizer uses exceeded the third quartile, the cropland we consider it intense use. The remaining cropland we consider to be light use. We converted the AEI source map to AEI per area and resampled it to 3 arcmin spatial resolution, assuming that the larger cells have the same AEI density as the smaller cells they encompass.

We built a pasture land-use intensity map by subdividing the pasture from HILDA+ based on GLOBIO 4[14]. We consider "grassland" as minimal use, "rangeland" as light use, and "pasture" as intense use. The GLOBIO 4 data was first reclassified to assign numeric values (minimal use=1, light use=2, intense use=3) to the three intensity levels and then resampled with the average method to align the resolution with the pasture map (3 arcmin, Fig. S1b). We rounded the averaged values to integers, by which we defined the pasture intensity for those areas overlapping with pasture in HILDA+. The remaining area in HILDA+ that is not covered by GLOBIO 4 was assigned as light use.

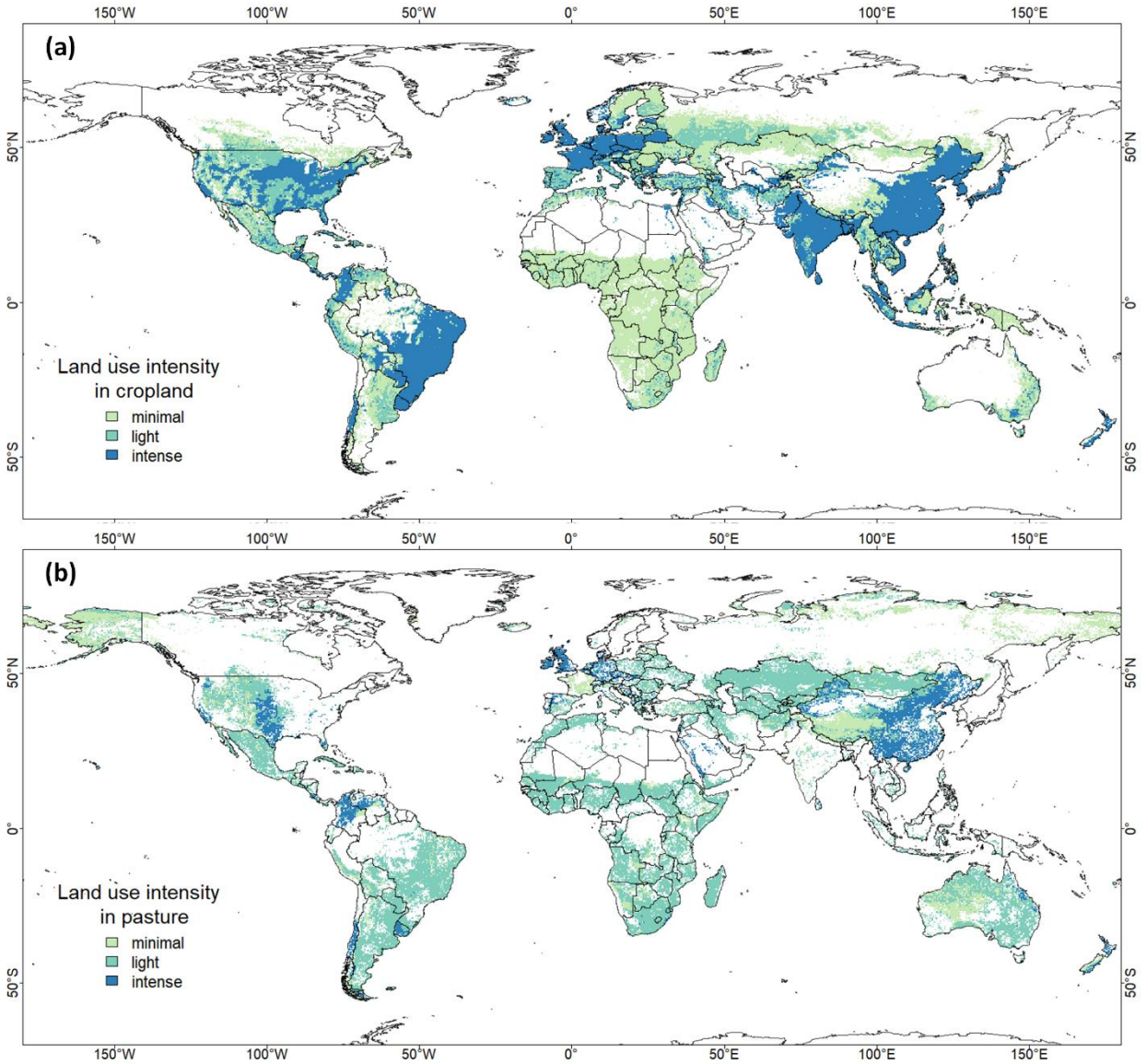

Fig. S3. Land use intensity in cropland (a) and pasture (b). Spatial resolution: 3 arcmin

With the obtained intensity maps (Fig. S3), we then mapped the aggregated, ecoregion-level CFs (based on average approach for land occupation, Scherer et al.[15]) across cropland and pasture by ecoregion[16], generating CF maps for cropland and pasture separately (Fig. S4).

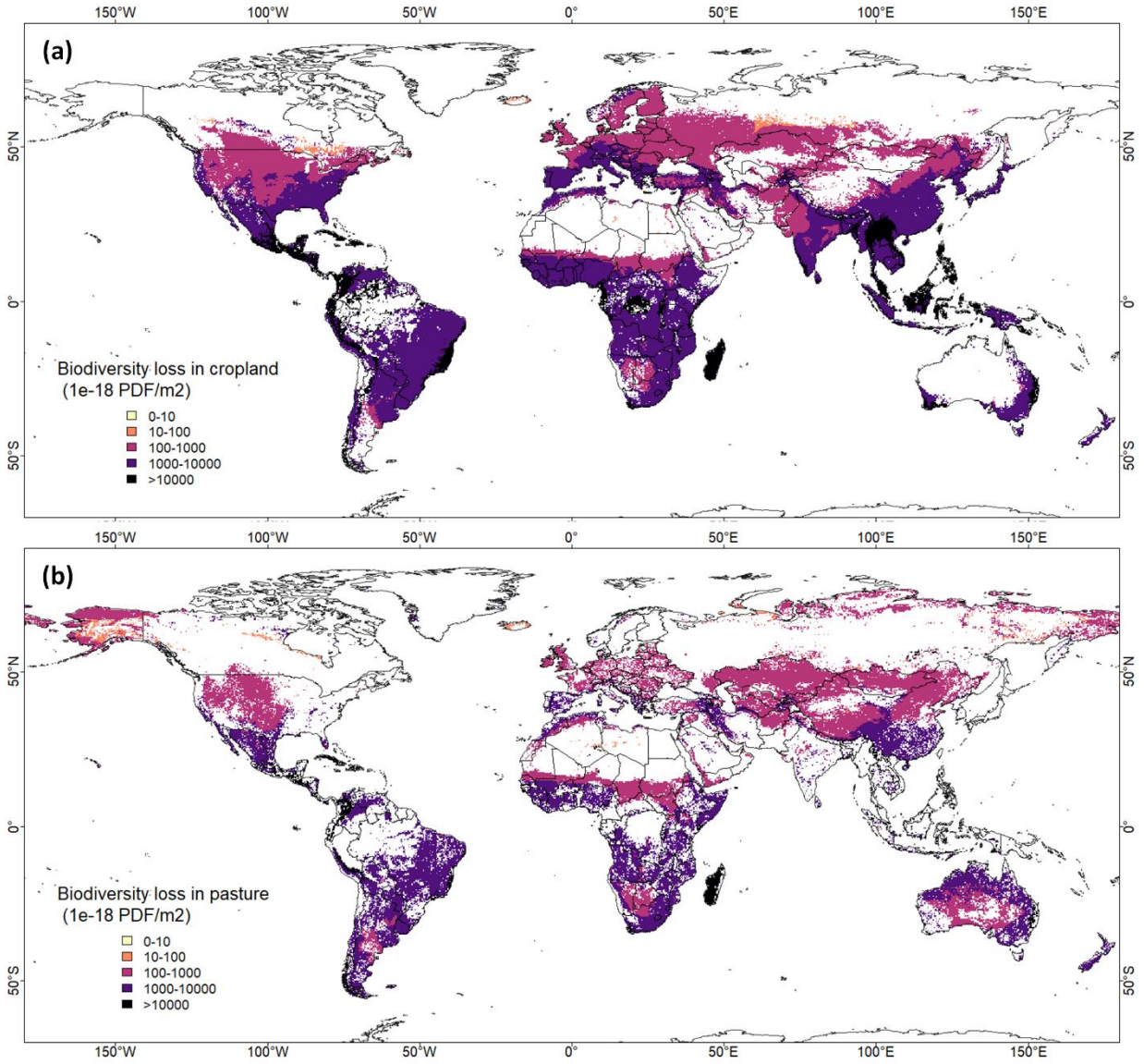

Fig. S4. Biodiversity loss intensity in cropland (a) and pasture (b). Spatial resolution: 3 arcmin

Combined loss density To combine carbon and biodiversity loss for each grid cell, we first normalized carbon and biodiversity loss (density) values using a cumulative distribution function using *ecdf()*[17]. For the observations for carbon or biodiversity loss in cropland or pasture, we use the observation dataset (excluding zero values) to compute a cumulative distribution function, from which we compute the probability (0-1) for each grid cell that a data point in the observations is less than or equal to it. We then assigned the returned cumulative probability to each grid cell. By doing this, we normalized each loss to a unitless number with a range of 0 to 1. The normalized value indicates its relative loss magnitude across the loss in agricultural land, with 1 representing the highest level of loss. Then, we averaged the normalized carbon and biodiversity losses into one single, unitless number, for cropland and pasture, separately (Fig. S5).

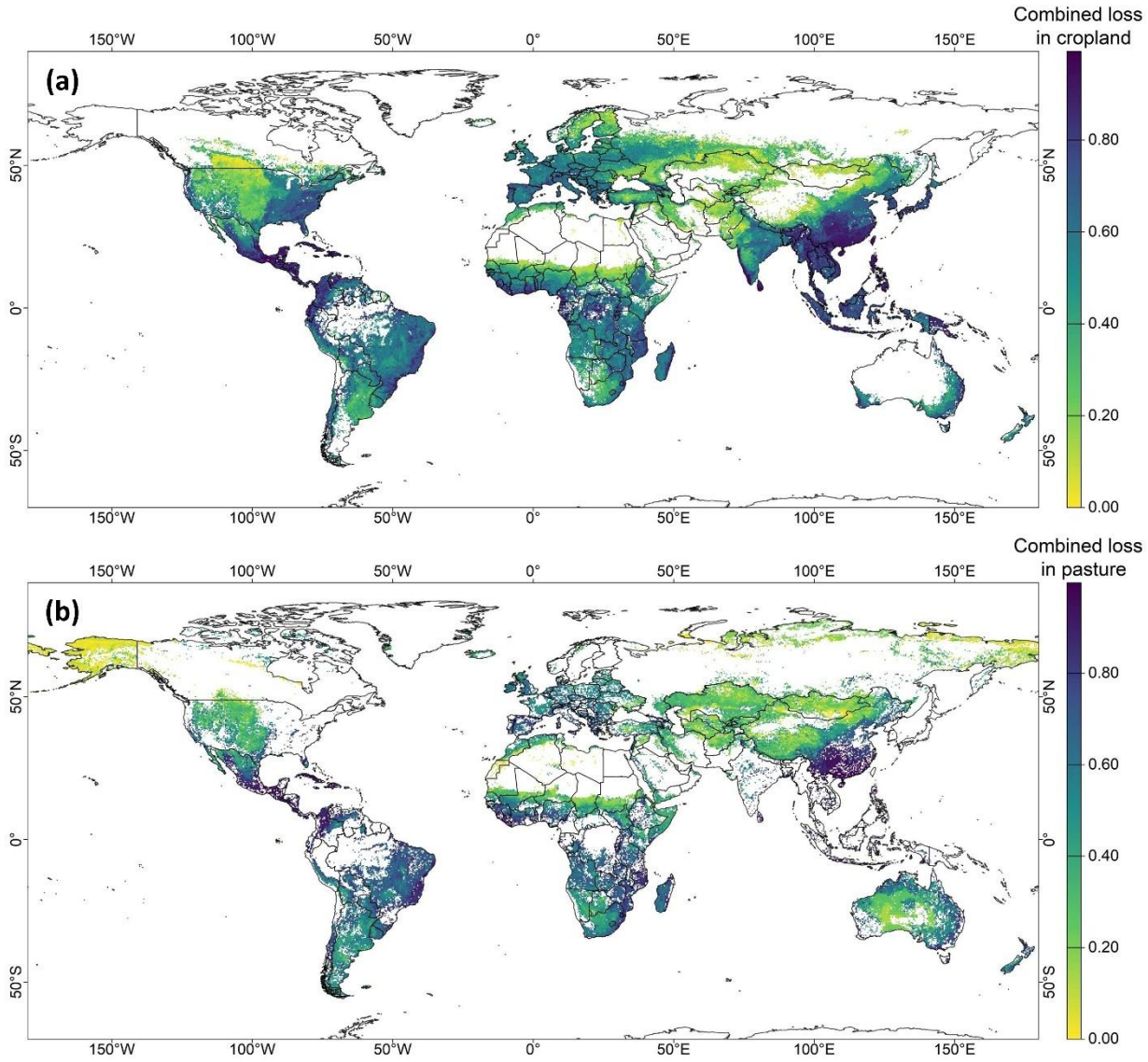

Fig. S5. Combined loss density in cropland and pasture. Spatial resolution: 3 arcmin

Linking impacts to FABIO We aggregated individual CROPGRIDS maps to align with the production items in FABIO. Because peppermint and pyrethrum are not included in any product category in FABIO, we linked 171 crops to 62 food product categories (see Table S1 for the detailed crop information in CROPGRIDS and Table S2 for the mapping relationships). We linked pasture-related pressure/impacts to the grazing item in FABIO. We used the country boundary shapefile data from GADM version 2.8[18]. We linked the spatial polygons to each region (except for the rest-of-the-world) in FABIO (see Table S3 for the region-related information), while we merged the remaining polygons for regions that are not included in FABIO and linked them to the rest-of-the-world.

We constructed land use impacts by linking map-based and country-specific land use areas to associated items in FABIO. We calculated the country-specific land use areas for each production item in FABIO by using zonal statistics function *exact_extract()* in the Terra package in R[19], with land

use maps and a FABIO-based country boundary shapefile as inputs. To obtain the map-based losses, we multiplied land use maps with loss density maps. With the same method, we constructed and connected impacts to FABIO for carbon loss, biodiversity loss and combined loss.

FABIO has several sub-categories in final demand, and we used the "food use" category throughout our analysis. In addition, FABIO provides two versions of the Z matrix that denotes inter-commodity input-output flows based on different allocation methods in production processes[20]. We used the matrix version with mass allocation.

Comparisons with other work Our findings are generally consistent with other work resulting total carbon and biodiversity losses in global agriculture. With all anthropogenic land use included, the cumulative land-use change (LUC) emissions are estimated at 250 ± 75 Pg C (between 1750 and 2022[21]). Based on the estimated total biomass carbon loss and the shares related to our land use scope, 312 Pg C with a range of 157 Pg C-487 Pg C can be derived from Erb et al.[4]. Our biomass carbon loss result is lower than the derived mean value, as we use current actual biomass stock maps from Xu et al.[3], whose estimate for the same year is at the lower bound of those datasets used in Erb et al.[4]. Comparing with Scherer et al.[15], our total biodiversity loss result (0.137 PDF) is close but lower than theirs (0.156 PDF). This is mainly because we account for cropland and pasture only, whereas Scherer et al.[15] applied the same CFs to global land use in 2015, including plantations, managed forests and urban land. We find 18% of food-related carbon and biodiversity loss embedded in international trade flows, which is in the range of findings from other studies looking at trade in all goods[22–26].

Other supplementary figures and tables

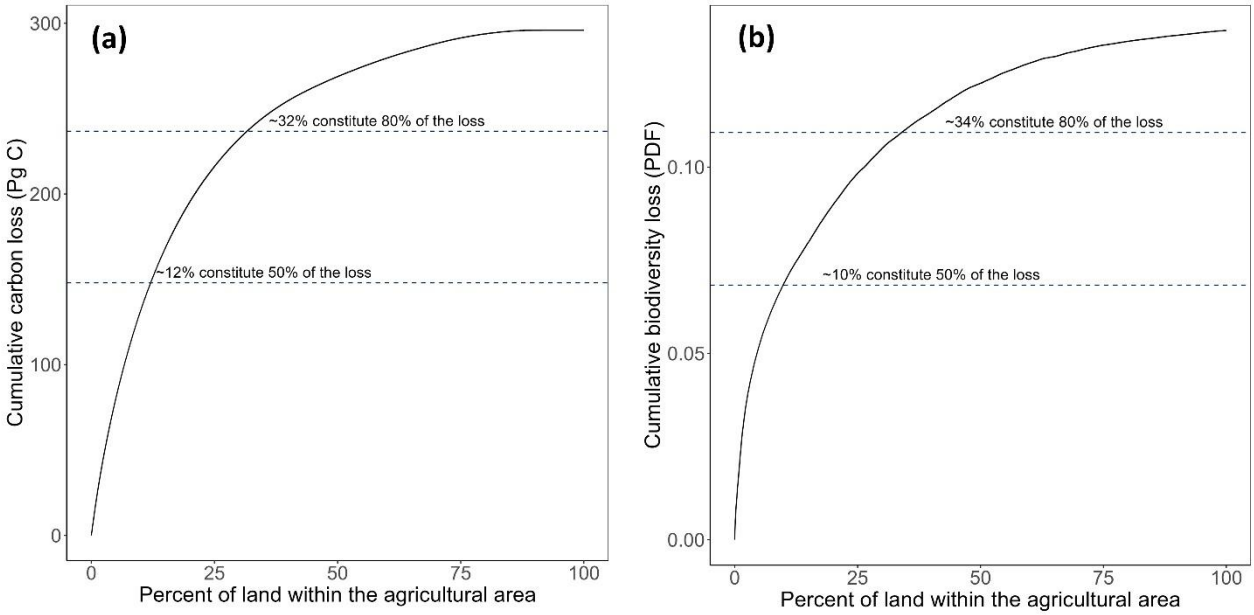

Fig. S6 Cumulative carbon loss (a) and biodiversity loss (b) based on land area. The blue dash lines mark the 50% and 80% of the cumulative loss.

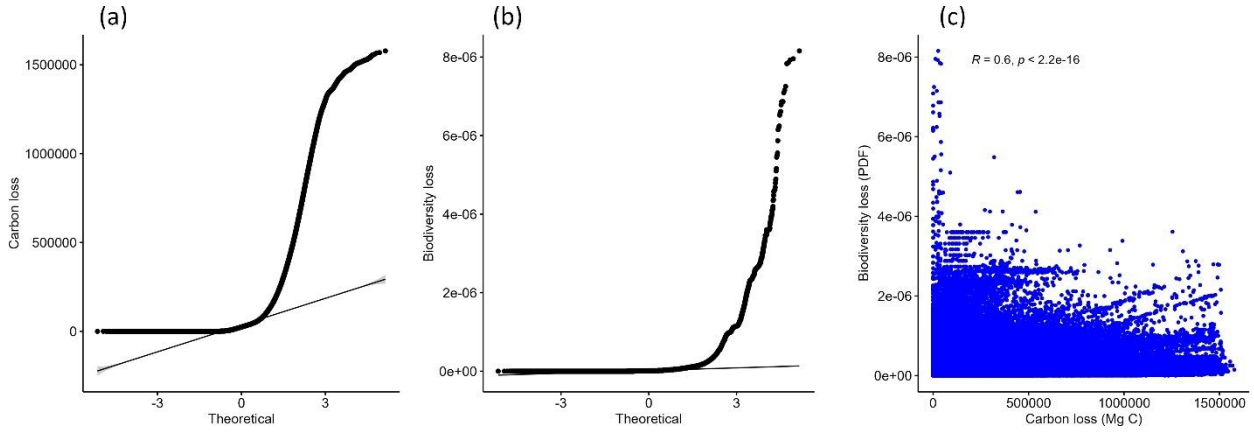

Fig. S7. Q-Q plot of carbon loss (a), biodiversity loss (b), and data distribution and Spearman's rank correlation coefficient of the two losses (c). Visual inspection is used to check the normality assumptions of the two datasets. If the data is normally distributed, the points in a Q-Q (quantile-quantile) plot will lie on a straight Q-Q line drawn through the 0.25th and 0.75th quantiles. The points in (a) and (b) deviate substantially from the straight line, indicating that the two data sets are not normally distributed. Therefore, we used non-parametric Spearman's rank correlation to explore the spatial association between the two losses. In (c), the blue dots represent the distribution of the two losses, and Spearman's rank correlation rho and p-value are shown on top.

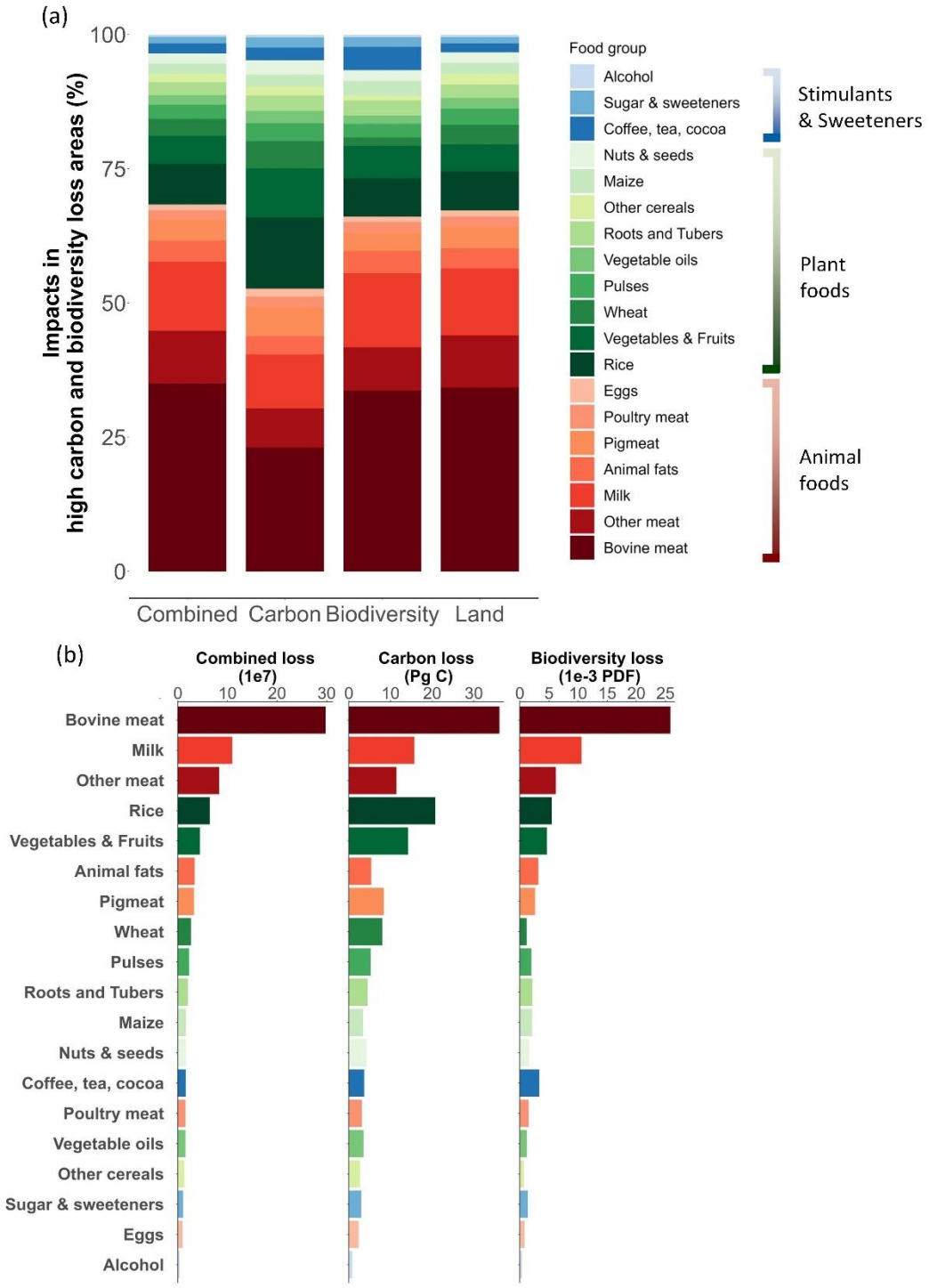

Fig. S8 The impact percentage of each food group in high carbon and biodiversity areas (a), and food group losses in combined loss, carbon loss and biodiversity loss in high carbon and biodiversity loss areas (b). Food groups in (b) are ranked in descending order by total combined loss.

Fig. S9 Food item losses in combined loss, carbon loss, biodiversity loss, and combined loss per area, per tonne and per kcal. Food items are ranked in descending order by total combined loss of the food group and then ordered by total combined loss of the item.

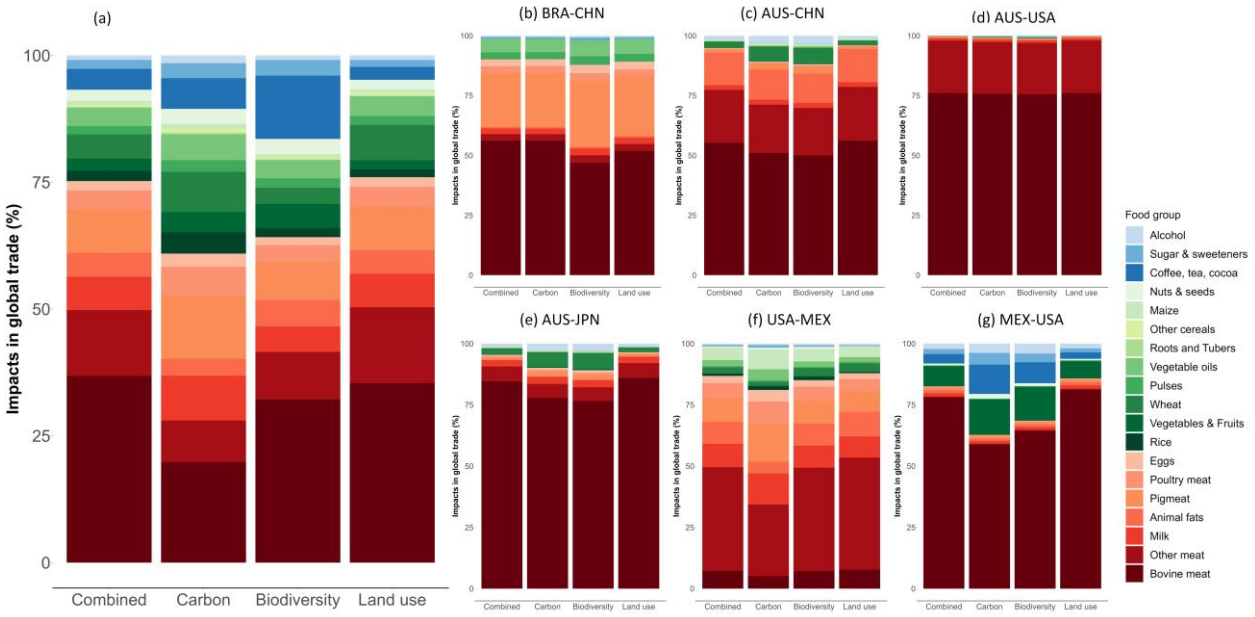

Fig. S10. Percentage of food group impacts embedded in global trade (a) and the largest trade relationships (b-g). Sub-figure names are using ISO3 codes for countries. The country in front of the hyphen is the exporting country.

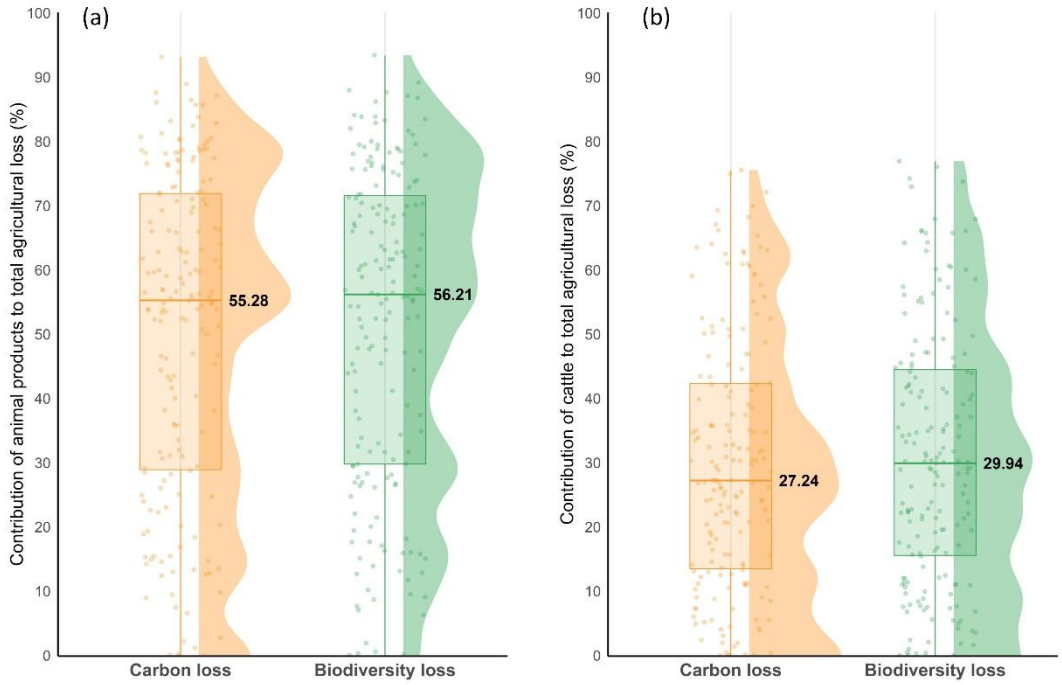

Fig. S11. Contribution of animal products (a) and cattle (b) to total agricultural loss at the national level. Dots represent the percentages for each country. The half-violins outline the distribution of results. The boxes represent the range from the first to the third quartile, and the horizontal lines within show the median. Qatar and Bahrain are not included in the charts given their milk data issue in FABIO.

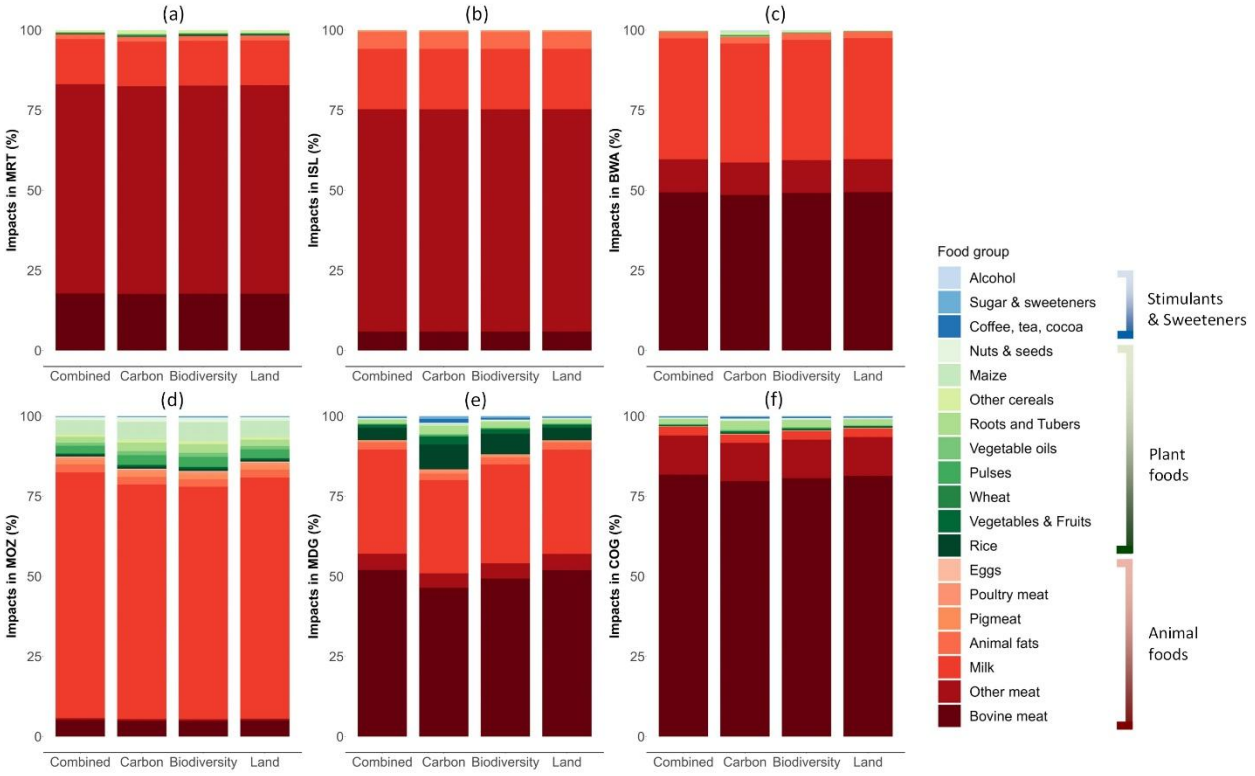

Fig. S12 Contribution of each food group in Mauritania (a), Iceland (b), Botswana (c), Mozambique (d), Madagascar (e) and Congo (f). Country names are using ISO3 codes.

Table S18. Largest five net importers and exporters.

Carbon loss (Pg C)								
	Country	Import	Export	**Net import**	Country	Import	Export	**Net export**
1	CHN	61.57	54.92	**6.64**	BRA	9.31	13.32	**4.01**
2	JPN	2.19	0.57	**1.62**	USA	11.28	13.61	**2.33**
3	ITA	2.40	1.37	**1.03**	AUS	2.01	4.19	**2.18**
4	KOR	1.37	0.38	**0.99**	UKR	1.92	3.52	**1.60**
5	GBR	4.14	3.31	**0.83**	IND	24.32	25.85	**1.53**
Biodiversity loss (1e-3 PDF)								
	Country	Import	Export	**Net import**	Country	Import	Export	**Net export**
1	CHN	12.25	8.19	**4.06**	BRA	8.37	12.76	**4.4**
2	USA	4.14	2.15	**1.99**	AUS	3.07	6.87	**3.8**
3	JPN	1.19	0.23	**0.96**	COL	5.57	6.4	**0.83**
4	KOR	0.76	0.05	**0.7**	ARG	1.58	2.29	**0.71**
5	GBR	0.48	0.06	**0.42**	MEX	4.85	5.39	**0.54**
Combined loss (1e6)								
	Country	Import	Export	**Net import**	Country	Import	Export	**Net export**

1	CHN	271.02	208.30	**62.72**	AUS	47.11	103.01	**55.91**
2	JPN	16.04	2.17	**13.88**	BRA	108.45	155.84	**47.39**
3	KOR	11.68	1.04	**10.65**	ARG	40.47	58.48	**18.00**
4	ZAF	48.40	41.39	**7.01**	PRY	4.95	12.11	**7.17**
5	EGY	5.66	0.44	**5.22**	NAM	7.13	13.54	**6.41**
Land use (million ha)								
	Country	Import	Export	**Net import**	Country	Import	Export	**Net export**
1	CHN	579.27	446.96	**132.31**	AUS	113.3	247.43	**134.14**
2	JPN	36.15	2.83	**33.32**	BRA	161.99	235.14	**73.15**
3	KOR	27.02	1.40	**25.62**	ARG	85.28	127.94	**42.67**
4	ZAF	96.25	78.71	**17.54**	CAN	19.48	38.83	**19.35**
5	VNM	21.02	8.71	**12.31**	USA	255.61	271.3	**15.68**

Table S19. Largest five transborder displacements and main driving foods.

Carbon (Pg C)						
	Loss country	Driving country	Value	Main driving foods		
1	BRA	CHN	1.78	Bovine meat	Pigmeat	Vegetable oils
2	USA	CHN	1.65	Pigmeat	Vegetable oils	Bovine meat
3	USA	MEX	0.80	Other meat	Pigmeat	Milk
4	MEX	USA	0.62	Bovine meat	Vegetables & Fruits	Coffee, tea, cocoa
5	AUS	CHN	0.48	Bovine meat	Other meat	Animal fats
Biodiversity (1e-3 PDF)						
	Loss country	Driving country	Value	Main driving foods		
1	BRA	CHN	1.83	Bovine meat	Pigmeat	Vegetable oils
2	AUS	CHN	0.78	Bovine meat	Other meat	Animal fats
3	MEX	USA	0.55	Bovine meat	Vegetables & Fruits	Coffee, tea, cocoa
4	AUS	USA	0.49	Bovine meat	Other meat	Milk
5	AUS	JPN	0.48	Bovine meat	Wheat	Other meat
Combined loss (1e6)						
	Loss country	Driving country	Value	Main driving foods		
1	BRA	CHN	21.67	Bovine meat	Pigmeat	Vegetable oils
2	AUS	CHN	11.98	Bovine meat	Other meat	Animal fats
3	AUS	USA	8.36	Bovine meat	Other meat	Milk
4	AUS	JPN	7.54	Bovine meat	Other meat	Milk
5	ARG	CHN	7.26	Bovine meat	Pigmeat	Vegetable oils
Land use (million ha)						
	Loss country	Driving country	Value	Main driving foods		
1	BRA	CHN	34.41	Bovine meat	Pigmeat	Vegetable oils
2	AUS	CHN	28.85	Bovine meat	Other meat	Animal fats
3	AUS	USA	20.47	Bovine meat	Other meat	Milk

4	AUS	JPN	18.18	Bovine meat	Other meat	Milk
5	ARG	CHN	15.58	Bovine meat	Pigmeat	Vegetable oils

References

1. Tang, F. H. M. *et al.* CROPGRIDS: a global geo-referenced dataset of 173 crops. *Sci Data* **11**, 413 (2024).
2. Winkler, K., Fuchs, R., Rounsevell, M. & Herold, M. Global land use changes are four times greater than previously estimated. *Nat Commun* **12**, 2501 (2021).
3. Xu, L. *et al.* Changes in global terrestrial live biomass over the 21st century. *Sci Adv* **7**, eabe9829 (2021).
4. Erb, K. H. *et al.* Unexpectedly large impact of forest management and grazing on global vegetation biomass. *Nature* **553**, 73–76 (2018).
5. Walker, W. S. *et al.* The global potential for increased storage of carbon on land. *Proceedings of the National Academy of Sciences* **119**, e2111312119 (2022).
6. Beyer, R. M., Hua, F., Martin, P. A., Manica, A. & Rademacher, T. Relocating croplands could drastically reduce the environmental impacts of global food production. *Commun Earth Environ* **3**, 49 (2022).
7. Searchinger, T. D., Wirsenius, S., Beringer, T. & Dumas, P. Assessing the efficiency of changes in land use for mitigating climate change. *Nature* **564**, 249–253 (2018).
8. West, P. C. *et al.* Trading carbon for food: Global comparison of carbon stocks vs. crop yields on agricultural land. *Proceedings of the National Academy of Sciences* **107**, 19645–19648 (2010).
9. Sun, Z. *et al.* Dietary change in high-income nations alone can lead to substantial double climate dividend. *Nat Food* **3**, 29–37 (2022).
10. Sanderman, J., Hengl, T. & Fiske, G. J. Soil carbon debt of 12,000 years of human land use. *Proceedings of the National Academy of Sciences* **114**, 9575–9580 (2017).
11. Scherer, L. *et al.* Biodiversity Impact Assessment Considering Land Use Intensities and Fragmentation. *Environ Sci Technol* **57**, 19612–19623 (2023).
12. Mehta, P. *et al.* Majority of 21 st century global irrigation expansion has been in water stressed regions (preprint). (2022) doi:10.31223/X5C932.
13. Lu, C. & Tian, H. Global nitrogen and phosphorus fertilizer use for agriculture production in the past half century: shifted hot spots and nutrient imbalance. *Earth Syst. Sci. Data* **9**, 181–192 (2017).

14. Schipper, A. M. *et al.* Projecting terrestrial biodiversity intactness with GLOBIO 4. *Glob Chang Biol* **26**, 760–771 (2020).

15. Scherer, L. *et al.* Biodiversity Impact Assessment Considering Land Use Intensities and Fragmentation. *Environ Sci Technol* **57**, 19612–19623 (2023).

16. Olson, D. M. *et al.* Terrestrial Ecoregions of the World : A New Map of Life on Earth. *Bioscience* **51**, 933–938 (2001).

17. R Core Team. Documentation for package 'stats' version 4.3.3. https://stat.ethz.ch/R-manual/R-devel/library/stats/html/00Index.html (2024).

18. GADM. GADM Version 2.8. https://gadm.org/data.html (2020).

19. Hijmans, R. J. *et al. Package 'Terra': Spatial Data Analysis*. https://cran.r-project.org/web/packages/terra/index.html (2024).

20. Bruckner, M. *et al.* FABIO - The Construction of the Food and Agriculture Biomass Input-Output Model. *Environ Sci Technol* **53**, 11302–11312 (2019).

21. Friedlingstein, P. *et al.* Global Carbon Budget 2023. *Earth Syst Sci Data* **15**, 5301–5369 (2023).

22. Chaudhary, A. & Kastner, T. Land use biodiversity impacts embodied in international food trade. *Global Environmental Change* **38**, 195–204 (2016).

23. Kitzes, J. *et al.* Consumption-Based Conservation Targeting: Linking Biodiversity Loss to Upstream Demand through a Global Wildlife Footprint. *Conserv Lett* **10**, 531–538 (2017).

24. Lenzen, M. *et al.* International trade drives biodiversity threats in developing nations. *Nature* **486**, 109–112 (2012).

25. Sun, Z., Behrens, P., Tukker, A., Bruckner, M. & Scherer, L. Global Human Consumption Threatens Key Biodiversity Areas. *Environ Sci Technol* **56**, 9003–9014 (2022).

26. Marques, A. *et al.* Increasing impacts of land use on biodiversity and carbon sequestration driven by population and economic growth. *Nat Ecol Evol* **3**, 628–637 (2019).